Compartmentalization in Nitroxide-Mediated Radical Polymerization in Dispersed Systems

Per B. Zetterlund[‡,§] and Masayoshi Okubo*[,‡,||]

Department of Chemical Science and Engineering, Faculty of Engineering, Kobe University, Kobe 657-8501, Japan, and Graduate School of Science and Technology, Kobe University, Kobe 657-8501, Japan

Received April 14, 2006; Revised Manuscript Received September 24, 2006

ABSTRACT: Modified Smith−Ewart equations were used to quantitatively investigate compartmentalization effects in nitroxide-mediated radical polymerization in dispersed systems. Calculations were carried out for the specific system 2,2,6,6-tetramethylpiperidinyl-1-oxy (TEMPO)/styrene at 125 °C with thermal initiation included in the model, and accounting for compartmentalization of both propagating radicals and nitroxide. For particles with diameter (d) less than approximately 60 nm, a reduction in particle size led to lower rate of polymerization, higher degree of livingness, and a higher number of activation−deactivation cycles experienced per chain to grow to a given degree of polymerization. These effects have their origin in the pseudo first-order deactivation rate coefficient increasing in proportion to d^{-3} with decreasing particle size. There were no significant effects of compartmentalization for particles with $d > 110$ nm. The results show that it is important to consider compartmentalization effects also on the deactivation reaction, and not only bimolecular termination.

Introduction

Radical polymerization has experienced a renaissance over the past decade as a result of the emergence of controlled/living radical polymerization (CLRP), which enables synthesis of polymers of predetermined molecular weight of narrow distribution and various complex architectures.[1,2] Research in CLRP has now expanded to application of these processes in the industrially important aqueous heterogeneous systems.[3−8] Aqueous heterogeneous systems are more complex than the corresponding homogeneous systems due to phase transfer events,[9] partitioning of reactants between the aqueous and organic phases,[10−12] and compartmentalization.[9,13−16]

The three most well-known CLRP techniques are nitroxide-mediated polymerization (NMP),[17,18] atom transfer radical polymerization,[19] and reversible addition−fragmentation chain transfer polymerization.[20] Control in NMP is achieved via reversible capping of propagating radicals with a suitable nitroxide.[2] The term "compartmentalization" encompasses effects arising from radicals located in different particles being unable to undergo reaction with one another (in the absence of phase transfer events), and the reaction rate between two radicals located in the same particle increasing with decreasing particle diameter. Compartmentalization is the origin of many characteristic features of conventional (i.e., not CLRP) emulsion polymerization, such as the usual formation of higher molecular weight polymer at higher rates than in the corresponding bulk polymerizations.[9] The kinetics of CLRP are very different from conventional radical polymerization processes, and it is not trivial to predict what the effects of compartmentalization, if any, are on a specific CLRP process in a dispersed system.

A general, rigorous understanding of compartmentalization effects in NMP has yet to emerge. In the case of 2,2,6,6-tetramethylpiperidinyl-1-oxy- (TEMPO-) based NMP of styrene (S), the experimental results are quite similar in bulk and miniemulsion,[21−29] suggesting that compartmentalization effects are not significant under the conditions employed. The literature contains various proposed rationales with respect to compartmentalization in dispersed NMP systems. It has been argued that the controlling effect of TEMPO overwhelms the propagating radical segregation effect,[22−24] that the rate of termination may decrease if particles are sufficiently small,[27] and that the rate of polymerization (R_p) will be low in a compartmentalized system because the frequency of activation is much lower than that of deactivation.[30]

Butte et al.[13] modeled miniemulsion NMP using modified Smith−Ewart equations[31] whereby compartmentalization of both propagating radicals and nitroxide were considered, including thermal initiation in the model. In the case of S/TEMPO at 125 °C, smaller particles resulted in less bimolecular termination, lower polydispersity (M_w/M_n), and lower R_p. These findings were rationalized by arguing that compartmentalization reduces the level of termination involving propagating radicals, but smaller particles leads to higher rates of termination of thermally generated radicals. Thermal initiation by S yields radicals in pairs,[32] and the rate of thermal initiation ($R_{i,th}$) is reduced due to geminate termination if the particles are sufficiently small.[13,24,33] Limited simulations were also carried out with a 10-fold increase in the rate of activation, also resulting in lower R_p and less termination for smaller particles.[13]

Charleux[34] reported simulations of miniemulsion NMP of S using SG1 (*N-tert*-butyl-*N*-(1-diethylphosphono-2,2-dimethylpropyl) nitroxide) at 90 °C (thermal initiation assumed negligible) based on the Smith−Ewart equations.[31] Compartmentalization was considered with respect to the propagating radicals, whereas compartmentalization effects on the deactivation step (i.e., the nitroxide) were not accounted for. It was assumed that the activation−deactivation equilibrium was the same as in a noncompartmentalized system (not assumed by Butte et al.[13]). It was found that smaller particles led to less bimolecular termination, higher R_p, less dead chains and higher polydisper-

* Corresponding author. Fax: +81-(0)78−8036161, E-mail: okubo@kobe-u.ac.jp.

† Part CCLXXII of the series "Studies on Suspension and Emulsion".

‡ Department of Chemical Science and Engineering, Faculty of Engineering, Kobe University.

§ E-mail: pbzttlnd@cx6.scitec.kobe-u.ac.jp.

|| Graduate School of Science and Technology, Kobe University.

10.1021/ma060841b CCC: $33.50
Published on Web 11/22/2006

Table 1. Parameter Values for 2,2,6,6-Tetramethylpiperidinyl-1-oxy- (TEMPO-) Mediated Radical Polymerization of Styrene at 125 °C

rate parameter	value
k_d (activation)	1.60×10^{-3} s^{-1} [36]
k_{da} (deactivation)	7.60×10^{7} M^{-1} s^{-1} [21,36]
k_p (propagation)	2.32×10^{3} M^{-1} s^{-1} [37]
k_t (termination)[a]	1.72×10^{8} M^{-1}s^{-1} [38]
$k_{i,th}$ (thermal initiation)[b]	1.70×10^{-10} M^{-2}s^{-1} [39]

[a] On the basis of termination rate $= 2k_t[P^\bullet]^2$. [b] On the basis of radical generation rate $= k_{i,th}[S]^3$.

sity (due to fewer activation−deactivation cycles).

There are significant gaps in the understanding of compartmentalization effects in NMP in dispersed systems, and conflicting views and theories have been presented in recent years. In particular, as discussed above, the very different results obtained by Charleux[34] and Butte et al.[13] stand out. The different results are apparently caused by the following: (i) the inclusion or not of thermal initiation (Butte et al.[13] included thermal initiation; Charleux[34] did not) and/or (ii) inclusion of compartmentalization of nitroxide in the model (Butte et al.[13] included nitroxide compartmentalization; Charleux[34] did not). Several years have passed since these publications appeared, but the matter has not been resolved. In view of the fact that CLRP in dispersed media is receiving increasing attention recently due to the importance of successfully applying CLRP in these industrially important systems,[3−8] we revisited the subject of compartmentalization effects on NMP. In the present investigation, extensive simulations and detailed analyses are carried out based on the modified Smith−Ewart equations used by Butte et al.,[13] thus accounting for compartmentalization effects on both propagating radicals and nitroxide. The influence of thermal initiation is clarified by performing a range of simulations with and without thermal initiation. The present paper shows that there are significant effects of compartmentalization in NMP for sufficiently small particles (diameter < 110 nm for S/TEMPO at 125 °C) mainly due to particle size effects on the pseudo first-order rate coefficient for deactivation. It is demonstrated that it is crucial to consider compartmentalization effects on both propagating radicals and nitroxide.

Model Development

Homogeneous System. Homogeneous (bulk/solution) NMP was modeled using eqs 1−4.[2]

$$\frac{d[M]}{dt} = -k_p[P^\bullet][M] \quad (1)$$

$$\frac{d[PT]}{dt} = k_{da}[P^\bullet][T^\bullet] - k_d[PT] \quad (2)$$

$$\frac{d[T^\bullet]}{dt} = k_d[PT] - k_{da}[P^\bullet][T^\bullet] \quad (3)$$

$$\frac{d[P^\bullet]}{dt} = k_d[PT] + k_{i,th}[M]^3 - k_{da}[P^\bullet][T^\bullet] - 2k_t[P^\bullet]^2 \quad (4)$$

where M denotes monomer, PT denotes alkoxyamine, $T^\bullet$ is nitroxide, $P^\bullet$ is a propagating radical, k_p is the propagation rate coefficient, k_d is the dissociation rate coefficient of PT, k_{da} is the deactivation rate coefficient, k_t is the termination rate coefficient, and $k_{i,th}$ is the rate coefficient for thermal initiation (values listed in Table 1). Chain-length dependence of rate coefficients[35] was not included in the model. The simulations were not taken beyond 10% monomer conversion, and conversion-independent values of k_p, k_t and k_{da} could therefore be used.[40,41] All simulations were carried out with $[S]_0 = 8.71$ M (refers to particle phase in dispersed system).

Dispersed System. To account for compartmentalization effects on both $[P^\bullet]$ and $[T^\bullet]$, the Smith−Ewart equations[31] extended to two dimensions derived by Butte et al.[13] were employed, assuming that the number of particles remains constant with conversion and that the particles constitute the sole locus of polymerization. The modified Smith−Ewart equations[13] describing the number fraction of particles N_i^j (particles containing $i P^\bullet$ and $j T^\bullet$) read as follows:

$$\frac{dN_i^j}{dt} = N_A \upsilon_p k_d[PT]\{N_{i-1}^{j-1} - N_i^j\} + 0.5k_{i,th}[S]^3 N_A \upsilon_p \{N_{i-2}^j - N_i^j\} + \frac{k_t}{N_A \upsilon_p}\{(i+2)(i+1)N_{i+2}^j - (i)(i-1)N_i^j\} + \frac{k_{da}}{N_A \upsilon_p}\{(i+1)(j+1)N_{i+1}^{j+1} - (i)(j)N_i^j\} \quad (5)$$

The "2" appearing in the termination term in eq 4 is absent in eq 5, because one termination event (which consumes two radicals, thus "2" in eq 4) leads to the disappearance of one particle and the generation of another (e.g., $N_3^6 \rightarrow N_1^6$). For the same reason, there is a factor "0.5" in the term for thermal initiation in eq 5 but not in eq 4 (the value of $k_{i,th}$ used is defined as $R_{i,th} = k_{i,th}[M]^3$). The average numbers of $P^\bullet$ ($\bar{n}_p$) and $T^\bullet$ ($\bar{n}_T$) per particle are ($\Sigma_i \Sigma_j N_i^j = 1$):

$$\bar{n}_p = \sum_i \sum_j i N_i^j \quad (6)$$

$$\bar{n}_T = \sum_i \sum_j j N_i^j \quad (7)$$

No assumption was made with regards to whether the system follows zero-one kinetics[9] or not. The overall concentrations of $P^\bullet$ and $T^\bullet$ per unit volume organic phase are given by

$$[P^\bullet] = (N_A \upsilon_p)^{-1} \sum_i \sum_j i N_i^j \quad (8)$$

$$[T^\bullet] = (N_A \upsilon_p)^{-1} \sum_i \sum_j j N_i^j \quad (9)$$

The concentration of the noncompartmentalized species S is obtained from eqs 1 and 8. Compartmentalization of both $P^\bullet$ and $T^\bullet$ is considered when computing [PT]:

$$\frac{d[PT]}{dt} = \frac{k_{da}}{(N_A \upsilon_p)^2} \sum_i \sum_j ij N_i^j - k_d[PT] \quad (10)$$

The system of equations was solved by numerical integration using the Backward Euler integration algorithm[42] with a step size of 1 s. Great care was taken to ensure minimization of any numerical errors in the simulations. The total number of particles in the simulated system was ensured to remain constant with time in all cases.

Phase Transfer. In conventional S emulsion polymerization, chain transfer to monomer followed by exit and reentry are significant kinetic events if the polymer particles are sufficiently small.[9] The number of chain transfer events per chain is much lower in CLRP, because the degree of polymerization is lower in CLRP than in a conventional system. However, considered over the total number of chains, it cannot be excluded that chain transfer to monomer exerts some influence on $\bar{n}_p$. An additional

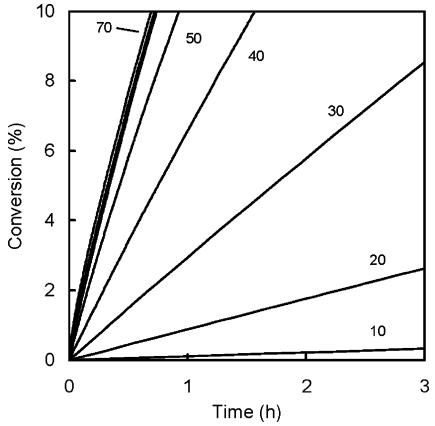

Figure 1. Simulated conversion vs time (eqs 1, 5, 8 and 10) for different particle diameters (in nm as indicated) for 2,2,6,6-tetramethylpiperidinyl-1-oxy- (TEMPO-) mediated radical polymerization of styrene at 125 °C (thermal initiation included; $[PT]_0 = 0.02$ M; PT = polystyrene−TEMPO macroinitiator). The thick line denotes bulk conditions (eqs 1−4). All rate coefficients are listed in Table 1.

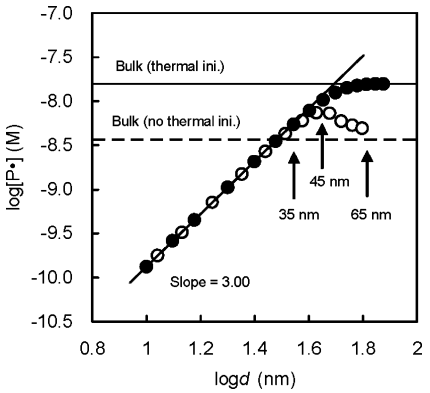

Figure 2. Simulated (eqs 1, 5, 8 and 10) propagating radical concentrations ([P•]; 10% styrene conversion) for 2,2,6,6-tetramethylpiperidinyl-1-oxy- (TEMPO-) mediated radical polymerization of styrene ($[PT]_0 = 0.02$ M; PT = polystyrene−TEMPO macroinitiator) with (●) and without (○) thermal initiation at 125 °C for different particle diameters (d). The horizontal lines show [P•] in the corresponding bulk systems (eqs 1−4) at 10% conversion. All rate coefficients are listed in Table 1.

complication is nitroxide partitioning between particles and aqueous phase.[11,43,44] The significance of this process depends on the particular nitroxide. In the case of S/TEMPO at 135 °C, partitioning to the aqueous phase is relatively insignificant; $[TEMPO]_{org}/[TEMPO]_{aq} = 98.8$.[45] Phase transfer events are not included in the present model (although inclusion is trivial and will be investigated in a forthcoming publication) in order to clearly expose the effects of compartmentalization.

Results and Discussion

Rate of Polymerization. Simulated conversion−time curves for TEMPO-mediated miniemulsion radical polymerization of S at 125 °C using a poly(S)-TEMPO (PT) macroinitiator ($[PT]_0 = 0.02$ M) for different particle diameters (d) are displayed in Figure 1. The rate of polymerization (R_p) decreases dramatically with decreasing particle size. These results are very similar to those reported by Butte et al.[13] for the same system, who proposed that the low R_p was caused by increased rates of geminate termination of thermal radicals generated in pairs. Results of simulations with and without thermal initiation are plotted as log[P•] vs log d (for reasons explained below) at 10% conversion in Figure 2 (R_p is proportional to [P•]). R_p decreases dramatically with decreasing d also in the absence of thermal initiation, and the low R_p is thus not related to the efficiency of thermal initiation for $d < 35$ nm. In fact, [P•] is not affected at all by thermal initiation for $d < 35$ nm (Figure 2). In the presence of thermal initiation, [P•] increases with increasing d and approaches the corresponding bulk value at $d > 65$ nm. In the absence of thermal initiation, there is a maximum in [P•] at approximately 45 nm.

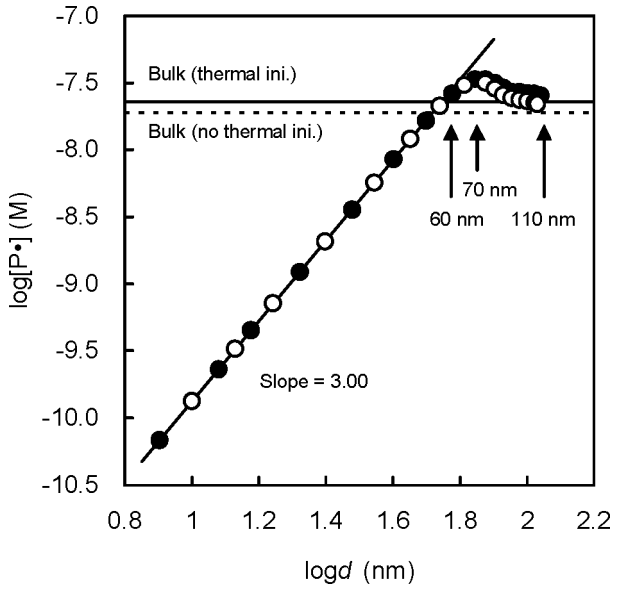

Figure 3. Simulated (eqs 1, 5, 8 and 10) propagating radical concentrations ([P•]; polymerization time = 1 min) for 2,2,6,6-tetramethylpiperidinyl-1-oxy- (TEMPO-) mediated radical polymerization of styrene at 125 °C ($[PT]_0 = 0.02$ M; PT = polystyrene−TEMPO macroinitiator) for different particle diameters (d) with (●) and without (○) thermal initiation. The horizontal lines show [P•] in the corresponding bulk systems (eqs 1−4). All rate coefficients are listed in Table 1.

There is a slight increase in R_p relative to bulk at low conversion (<4%) in the presence of thermal initiation for $d =$ 70 nm (Figure 1). To probe this further, log[P•] vs log d at very low conversion (in the stationary state, not the pre-stationary state region) was examined with and without thermal initiation (Figure 3). For $d < 60$ nm, [P•] is independent of thermal initiation. Both with and without thermal initiation, [P•] passes through a maximum at approximately 70 nm, after which the bulk values are approached.

The values of $\bar{n}_p$ and $\bar{n}_T$ are displayed as functions of conversion (in the presence of thermal initiation) for different values of d in Figure 4. Both $\bar{n}_p$ and $\bar{n}_T$ decrease with decreasing particle size. It is apparent that the polymerization process is strongly influenced by particle size for sufficiently small particles. In the present system under the present conditions, there are no significant effects of compartmentalization for particles with $d > 110$ nm. All these observations will be rationalized below in terms of compartmentalization effects on the deactivation (P• + T•) and bimolecular termination (P• + P•) reactions.

Compartmentalization Effects on Deactivation and Termination. There are two separate and opposite effects of compartmentalization on bimolecular reactions: (i) Segregation of radicals, i.e., two radicals located in separate particles being unable to react with one another, leads to a reduction in bimolecular reaction rate. (ii) The reaction rate between two radicals located in the same particle increases with decreasing particle size (hereafter referred to as "confined space effect"), expressed in terms of the pseudo first-order rate coefficient $k/N_A\upsilon_p$ (k is the rate coefficient in $M^{-1}s^{-1}$). Experimental

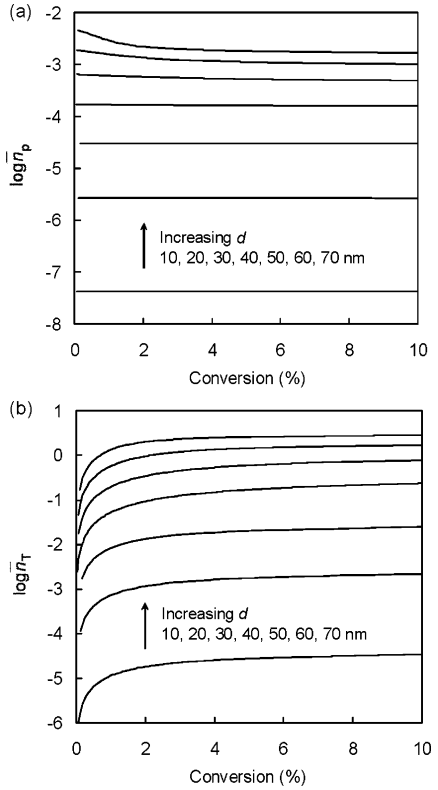

Figure 4. Simulated average number of propagating radicals ($\bar{n}_p$) and nitroxide molecules ($\bar{n}_T$) per particle vs conversion for 2,2,6,6-tetramethylpiperidinyl-1-oxy- (TEMPO-) mediated radical polymerization of styrene at 125 °C ($[PT]_0 = 0.02$ M; PT = polystyrene−TEMPO macroinitiator) with thermal initiation for different particle diameters (d). All rate coefficients are listed in Table 1.

evidence of the confined space effect is the increase in $\bar{n}_P$ with conversion usually observed in conventional radical emulsion polymerization of methyl methacrylate during interval II, caused by a continuous decrease in $k_t/N_A\upsilon_p$ as particles grow.[9,46]

To quantitatively assess the effects of compartmentalization on deactivation and termination separately, the deactivation rate (R_{da}^c; "c" denotes compartmentalization) and termination rate (R_t^c) predicted by the modified Smith−Ewart model were compared with the corresponding "homogeneous" deactivation rate (R_{da}^h; "h" denotes homogeneous) and termination rate (R_t^h) computed from the overall radical concentrations in the particle phase. R_{da}^h and R_t^h are thus the rates one would observe if the overall [P•] and [T•] were the same as in the compartmentalized system (i.e. eqs 8 and 9) and if the particles were "instantaneously combined" into a continuous bulk phase. The equations are

$$R_{da}^c = \frac{k_{da}}{(N_A\upsilon_p)^2}\sum_i\sum_j ijN_i^j \tag{11}$$

$$R_t^c = \frac{2k_t}{(N_A\upsilon_p)^2}\sum_i\sum_j i(i-1)N_i^j \tag{12}$$

$$R_{da}^h = k_{da}[P^\bullet][T^\bullet] \tag{13}$$

$$R_t^h = 2k_t[P^\bullet]^2 \tag{14}$$

where [P•] and [T•] are obtained from eqs 8 and 9. Note that the "2" in eq 12 (which is not present in the termination term in eq 5) is now necessary because we are here counting P• and not particles.

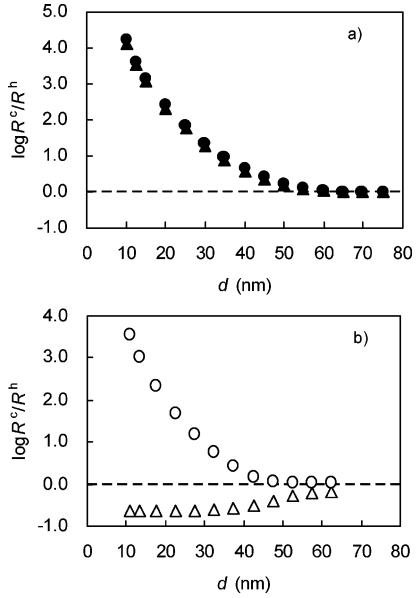

Figure 5. Ratios of simulated "compartmentalized" (eqs 11, 12) and "homogeneous" (eqs 13 and 14) deactivation (●, ○) and termination (▲, △) rates for 2,2,6,6-tetramethylpiperidinyl-1-oxy- (TEMPO-) mediated radical polymerization of styrene in the presence (a; ●, ▲) and absence (b; ○, △) of thermal initiation at 125 °C ($[PT]_0 = 0.02$ M; PT = polystyrene−TEMPO macroinitiator) at 10% styrene conversion for different particle diameters. R superscripts: c = compartmentalized; h = homogeneous. The dotted lines indicate $R^c = R^h$. All rate coefficients are listed in Table 1.

The quantities R_{da}^c/R_{da}^h (referred to as the relative deactivation rate) and R_t^c/R_t^h (referred to as the relative termination rate) were examined as functions of d for the conditions corresponding to the data in Figure 5 (10% conversion) and Figure 6 (polymerization time = 1 min.). The data in Figure 5a reveal that in the presence of thermal initiation, the relative deactivation and termination rates are affected in similar manners by compartmentalization. For $d < 60$ nm, the relative deactivation and termination rates increase strongly with decreasing d. These increases both originate in the confined space effect; smaller particle size leads to increases in the respective pseudo first-order rate coefficients, $k_{da}/N_A\upsilon_p$ and $k_t/N_A\upsilon_p$. The relative deactivation rate increases with decreasing d also in the absence of thermal initiation (Figure 5b). However, the relative termination rate exhibits an entirely different behavior in the absence of thermal initiation; $R_t^c/R_t^h = 0.24$ for $10 \le d \le 30$ nm, and gradually approaches unity as d increases.

The effects of particle size on R_{da}^c/R_{da}^h and R_t^c/R_t^h at the initial stage (polymerization time = 1 min.; Figure 6) are similar to at 10% conversion (Figure 5). In the presence of thermal initiation, both R_{da}^c/R_{da}^h and R_t^c/R_t^h increase with decreasing d (for the same reason as described above). In the absence of thermal initiation, $R_t^c/R_t^h = 0.24$ for $d < 55$ nm.

The origin of the maxima in [P•] (Figures 2 and 3) can now be explained. For large d, both the deactivation and the termination rate are the same as in the corresponding noncompartmentalized system, i.e. $R_{da}^c/R_{da}^h = R_t^c/R_t^h = 1$. As d decreases, R_{da}^c/R_{da}^h increases (*i.e.* the confined space effect on deactivation causes [P•] to decrease relative to the noncompartmentalized case) and R_t^c/R_t^h decreases (i.e. segregation causes [P•] to increase relative to the noncompartmentalized case). These two opposing effects result in a maximum in [P•]. This is clearly illustrated in the inset in Figure 6a; the maximum in [P•] at $d = 70$ nm (Figure 3) coincides with the minimum in R_t^c/R_t^h, the effect of which on [P•] is stronger than that of the

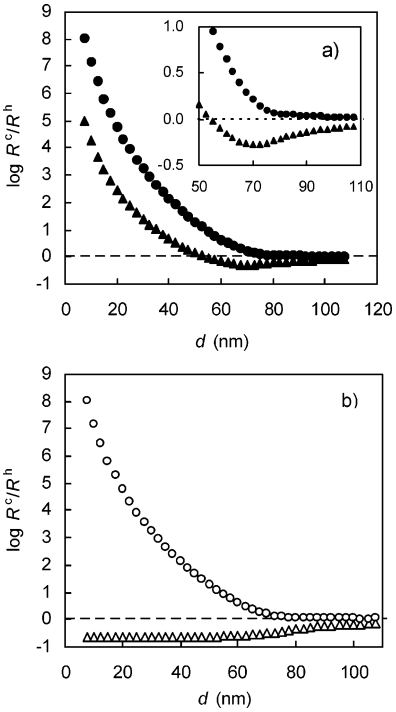

Figure 6. Ratios of simulated "compartmentalized" (eqs 11 and 12) and "homogeneous" (eqs 13 and 14) deactivation (●, ○) and termination (▲, △) rates for 2,2,6,6-tetramethylpiperidinyl-1-oxy- (TEMPO-) mediated radical polymerization of styrene in the presence (a; ●, ▲) and absence (b; ○, △) of thermal initiation at 125 °C ($[PT]_0 = 0.02$ M; PT = polystyrene−TEMPO macroinitiator) at polymerization time of 1 min R superscripts: c = compartmentalized; h = homogeneous. The dotted lines indicates $R^c = R^h$. All rate coefficients are listed in Table 1.

increase in deactivation rate relative to the noncompartmentalized system.

The termination rate as a function of d is very strongly affected by thermal initiation (Figures 5 and 6). In the absence of thermal initiation, segregation of propagating radicals is the dominant effect of compartmentalization on termination, resulting in a reduction in termination rate relative to bulk. In the presence of thermal initiation, there is a significant contribution toward the overall termination rate by geminate termination of thermal radicals generated in pairs (geminate termination is rapid in small particles[13,24,33] due to the confined space effect, i.e. the high value of $k_t/N_A\upsilon_p$, and the model does not distinguish between thermal radicals and propagating radicals generated by dissociation of PT), and the net effect for sufficiently small particles ($d <$ approximately 60 nm) is an increase in termination rate relative to bulk. The reason that [P•] is not affected by thermal initiation for sufficiently small particles (Figures 2 and 3) is that under such conditions geminate termination of thermal radicals is so fast that the contribution toward [P•] is negligible.

The deactivation rate would in principle also be expected to be influenced by segregation of P• and T• as well as by the confined space effect. However, it is apparent that the confined space effect is by far dominant (Figures 5 and 6; otherwise the slope would not be 3 in Figures 2 and 3—discussed in the next section), which is a result of generation of P• and T• in the same particle (in complete analogy with the termination rate increasing with decreasing d in the presence of thermal initiation). Another reason for the lack of a segregation effect on deactivation would be if $\bar{n}_T$ is sufficiently high (in the same way as there is no segregation effect on propagation because there is a very high number of S per particle), but this situation is not applicable here because of the low $\bar{n}_T$ (Figure 4).

Retardation by Enhanced Deactivation. It has been outlined above that the low R_p for very small particles ($d <$ approximately 35 nm) is due to the confined space effect on deactivation, i.e. on the term $k_{da}/N_A\upsilon_p$ (s^{-1}) in eq 5. For such small particles, the vast majority of activation events (approximately 98% for $d = 30$ nm at 10% conv.) occur in particles containing neither T• nor P•; $\bar{n}_T \approx 0.02$ and $\bar{n}_p \approx 4 \times 10^{-9}$ for $d = 30$ nm at 10% conversion. Thus, on the basis of the assumptions that (*i*) $N_0^0 + N_1^1 = N_{tot}$, and (*ii*) the rate of bimolecular termination is negligible, the following equations can be derived for a fixed organic volume:

$$N_0^0 + N_1^1 = N_{tot} \tag{15}$$

where N_{tot} is the total number of particles. The rate of change of N_1^1 with time is given by

$$\frac{dN_1^1}{dt} = N_A\upsilon_p k_d[PT]N_0^0 - \frac{k_{da}}{N_A\upsilon_p}N_1^1 \tag{16}$$

The term in eq 16 for deactivation can be derived from the deactivation term for N_i^j in eq 5, with $i = j = 1$. Application of the quasi steady-state assumption $dN_1^1/dt = 0$ yields

$$N_1^1 = \frac{(N_A\upsilon_p)^2 k_d[PT]N_0^0}{k_{da}} \approx \frac{(N_A\upsilon_p)^2 k_d[PT]N_{tot}}{k_{da}} \qquad (N_0^0 \approx N_{tot}) \tag{17}$$

On the basis of assumptions i and ii, the overall R_p (not per particle) is given by

$$R_p = k_p[M][P^\bullet] = \frac{k_p[M](N_1^1/N_{tot})}{N_A\upsilon_p} = \frac{k_p[M]k_d[PT]N_A\upsilon_p}{k_{da}} \tag{18}$$

At a given conversion ([M] and [PT] constant), a simplified form of eq 18 is

$$[P^\bullet] = C\upsilon_p = C\frac{\pi d^3}{6} \tag{19}$$

$$\log [P^\bullet] = \text{constant} + 3\log d \tag{20}$$

where C is a constant equal to $(k_d[PT]N_A)/k_{da}$. It follows that when assumptions i and ii hold, a plot of log[P•] vs log d should give a straight line with slope 3. This is indeed what is obtained (Figures 2 and 3); perfect linearity and a slope of 3.00 is observed for $d \leq 35$ nm. As d increases beyond 35 nm, log[P•] gradually begins to deviate from the straight line. This is because if the particle size is not sufficiently small, a significant fraction of activation events occur in particles that already contain T• and/or P•, and moreover, thermal initiation or another activation event may occur (both rates of which increase per particle with increasing particle size) prior to coupling of the original P• and T•. In other words, if the particles are "too large", assumptions i and ii do not hold.

It is also important to realize that the overall frequency of activation is independent of particle size, unlike in a conventional nonliving emulsion polymerization, where exit/entry events (corresponding to deactivation and activation, respectively) are strongly affected by particle size. The overall frequency of activation events is proportional to the total volume of the organic phase (i.e., the total number of PT), and is not a function of particle size. Thus, under conditions when eqs 18 and 19 are valid, even if the particle volume is increased (and

thus the number of particles reduced, keeping the total organic volume constant), N_1[1] remains the same.

An alternative way to visualize the scenario described by eqs 18 and 19 is that R_p is proportional to the number of monomer units added per activation−deactivation cycle, which is in turn proportional to the inverse of the pseudo first-order rate coefficient for deactivation ($N_A\upsilon_p$)/k_{da} (s^{-1}) in a particle that contains 1P• and 1T• (i.e., this is no longer true if the particles are "too large"). This accounts for the proportionality between [P•] and υ_p, and thus the slope of 3.00 in Figures 2 and 3.

In the presence of thermal initiation, R_p decreases due to enhanced rates of deactivation and geminate termination of thermal radicals (both due to the confined space effect) with decreasing particle size in the region d = 110 to 35 nm (Figure 2). When d decreases below approximately 35 nm, the rate of thermal initiation is negligible (only a negligible fraction of thermal radicals initiate polymerization as opposed to undergo geminate termination), and the reduction in R_p as the particles size is decreased further is due to the rate of deactivation increasing with decreasing particle size (the confined space effect).

One might ask, how can it be concluded that the increased termination rate relative to bulk (Figures 5a and 6a) is not a factor in causing low R_p for small particles? In the absence of thermal initiation, the termination rate is lower than in bulk for d < 110 nm (Figure 6), and R_p is independent of thermal initiation for d < 35 nm (Figure 2). Therefore, it can be concluded that the increased termination rate relative to bulk in the presence of thermal initiation is due to the contribution toward the overall termination rate by termination of thermal radicals generated in pairs. Consequently, the increased termination rate relative to bulk in Figure 5a and 6a is not the cause of the low R_p for small particles, consistent with the above analysis based on eqs 18 and 19.

The completely different simulation results and conclusions reached by Butte et al.[13] and Charleux[34] can now be explained. The differences arise because Charleux did not include compartmentalization of the nitroxide in the model, and therefore the increase in $k_{da}/N_A\upsilon_p$ with decreasing particle size is not captured by the model. Butte et al.[34] argued that the low R_p for small particles was caused by increased rates of geminate termination of thermal radicals (the confined space effect). As shown above, this explanation is incomplete, because an increased rate of deactivation (due to the confined space effect) is also a major cause of retardation, especially for very small particles (d < approximately 60 nm; Figure 5a and 6a).

Effect of Macroinitiator Concentration. In homogeneous NMP at the stationary state, [P•] is independent of $[PT]_0$, and [T•] increases linearly with $[PT]_0$ ($[P^\bullet] = (R_{i,th}/2k_t)^{0.5}$ and $[T^\bullet] = K[PT]/[P^\bullet]$)[2,21] The dependence of [P•] on $[PT]_0$ in a dispersed system with d = 20 nm (i.e., in the d region where [P•] and [T•] are independent of thermal initiation) is displayed in Figure 7; [P•] increases linearly with $[PT]_0$, consistent with the rationale proposed above for the plot of log[P•] vs log d being linear with a slope of 3.00 for d < 35 nm. The value of [T•] increases exponentially with $[PT]_0$. This is because [T•] has two "components": (i) T• due to dissociation of PT before rapid deactivation occurs involving the same species ("geminate" deactivation) and (ii) T• accumulated due to termination. Because of the small particle size and low [T•] compared to bulk, $\bar{n}_T$ is very low ($\bar{n}_T = 1.6 \times 10^{-3}$ at 1200 s (0.7% conversion) for $[PT]_0$ = 0.05 M and d = 20 nm, with thermal initiation). Consequently, the vast majority of activation events (>99.8% in the specific example above) occur in particles where there are no T•, and the accumulation of T• has no significant effect on the deactivation kinetics. The slope of the log[P•] vs log d plot in the low d range remains 3 regardless of $[PT]_0$ (unless $[PT]_0$ is unreasonably high).

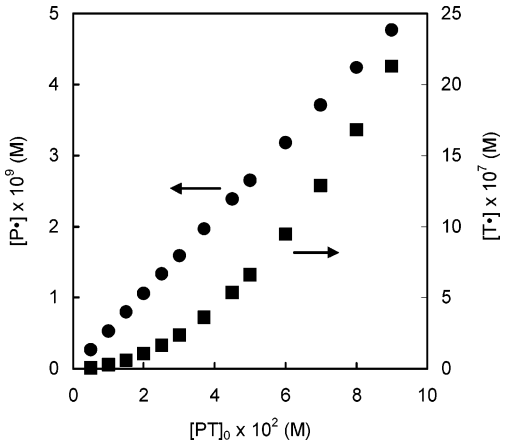

Figure 7. Simulated (eqs 1, 5, 8−10) values of propagating radical concentrations ([P•]) (●) and nitroxide concentrations ([T•]) (■) for 2,2,6,6-tetramethylpiperidinyl-1-oxy- (TEMPO-) mediated radical polymerization of styrene with thermal initiation at 125 °C in a dispersed system with d = 20 nm at polymerization time of 20 min. All rate coefficients are listed in Table 1.

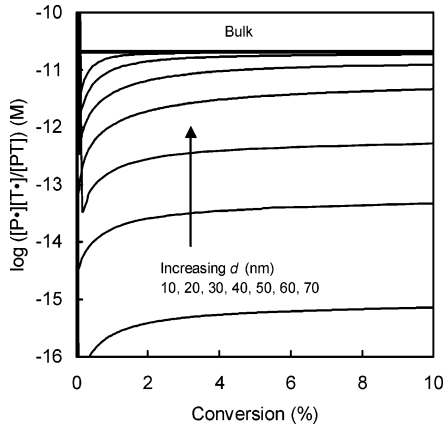

Figure 8. Simulated (eqs 1, 5, 8−10) values of ([P•][T•])/[PT] for 2,2,6,6-tetramethylpiperidinyl-1-oxy- (TEMPO-) mediated radical polymerization of styrene at 125 °C ($[PT]_0$ = 0.02 M; PT = polystyrene−TEMPO macroinitiator) for different particle diameters (d) with thermal initiation. P• = propagating radical; T• = TEMPO. All rate coefficients are listed in Table 1.

Equilibrium Constant (K). A question of interest is whether the equilibrium constant K (= ([P•][T•])/[PT]) for homogeneous conditions applies to NMP in compartmentalized systems, as assumed in the modeling by Charleux.[34] From the results presented above, it is already obvious that this is not the case. The quantity ([P•][T•])/[PT], calculated from simulated values of [P•], [T•], and [PT], deviates by orders of magnitude from the homogeneous literature value of $K = 2.1 \times 10^{-11}$ M for S/TEMPO at 125 °C (Figure 8).[21] For d = 40 nm, the effect of compartmentalization is a reduction in ([P•][T•])/[PT] by approximately 1 order of magnitude due to the confined space effect on deactivation. It is of interest to note that the maximum in [P•] at 70 nm (Figures 2 and 3) has no effect on the value of ([P•][T•])/[PT], which is the same as in bulk. The maximum is caused by a reduction in k_t due to segregation whereas the deactivation rate is only marginally affected, and k_t does not influence ([P•][T•])/[PT], which is determined by the relative rates of activation and deactivation (in bulk, $K = k_d/k_{da}$).

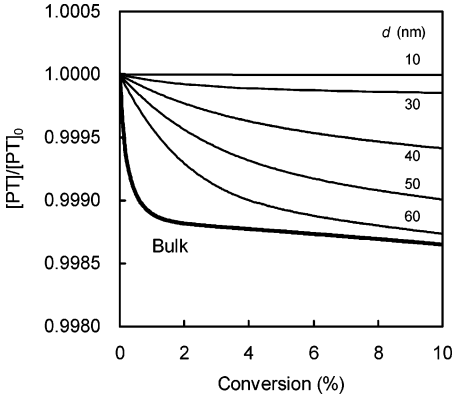

Figure 9. Simulated (eqs 1, 5, 8 and 10) values of fraction of alkoxyamine (rel. to initial amount) as a function of conversion for 2,2,6,6-tetramethylpiperidinyl-1-oxy- (TEMPO-) mediated radical polymerization of styrene at 125 °C ($[PT]_0 = 0.02$ M; PT = polystyrene−TEMPO macroinitiator) for different particle diameters (d) with thermal initiation. Thick line: Bulk conditions (eqs 1−4). All rate coefficients are listed in Table 1.

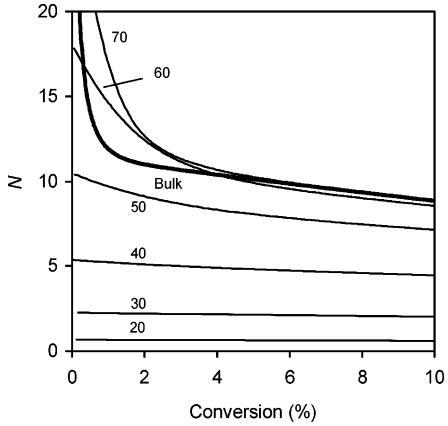

Figure 10. Simulated number of propagation events per activation−deactivation cycle for an individual chain (N) vs conversion for 2,2,6,6-tetramethylpiperidinyl-1-oxy- (TEMPO-) mediated radical polymerization of styrene at 125 °C ($[PT]_0 = 0.02$ M; PT = polystyrene−TEMPO macroinitiator) for different particle diameters (d; indicated in figure in nm) with thermal initiation. All rate coefficients are listed in Table 1.

Livingness. The fractional alkoxyamine concentration is plotted vs conversion in Figure 9 for S/TEMPO at 125 °C with thermal initiation for different particle sizes, revealing that the degree of livingness increases with decreasing particle size. In the presence of thermal initiation, the overall termination rate increases (relative to bulk) with decreasing particle size (Figures 5a and 6a). However, as mentioned earlier, this is due to the contribution by geminate termination of thermal radicals, which does not result in loss of PT. In the absence of thermal initiation (Figures 5b and 6b), the termination rate decreases with decreasing particle size due to segregation of P$^\bullet$, and this is the origin of the livingness increasing with decreasing d.

Polydispersity (M_w/M_n). In ideal CLRP (absence of termination, transfer and other side reactions), M_w/M_n is dictated by the number of activation−deactivation cycles that occur as polymer chains grow to their final molecular weight;[2] M_w/M_n decreases with increasing number of cycles for a given molecular weight. The number of propagation events per activation−deactivation cycle for an individual chain (N) was calculated from the ratio of propagation rate to deactivation rate:

$$N = \frac{k_p[M][P^\bullet]}{(N_A v_p)^{-2} k_{da} \sum_i \sum_j ijN_i^j} = \frac{k_p[M](N_A v_p)^{-1} \sum_i \sum_j iN_i^j}{(N_A v_p)^{-2} k_{da} \sum_i \sum_j ijN_i^j} = \frac{k_p[M] \sum_i \sum_j iN_i^j}{(N_A v_p)^{-1} k_{da} \sum_i \sum_j ijN_i^j} \quad (21)$$

where $(N_A v_p)^{-1} \sum_i \sum_j iN_i^j = [P^\bullet]$. For $d \leq 50$ nm, N decreases with decreasing particle size due to the increase in deactivation rate (Figure 10). A higher deactivation rate leads to fewer monomer units incorporated per activation−deactivation cycle, and thus a higher number of activation−deactivation cycles is required to reach a given molecular weight. In the computation of N, termination is not excluded (because termination affects [P$^\bullet$] in eq 21), and it follows that the maximum in [P$^\bullet$] at 70 nm (Figure 3) influences N. This is the reason N for $d = 60$ and 70 nm are higher than in bulk at low conversion. The values of N approach the bulk value at approximately 4% conversion, consistent with the maximum in [P$^\bullet$] appearing at low conversion (Figure 3; polymerization time = 1 min) but not at 10% conversion (Figure 2). N decreases with increasing conversion as T$^\bullet$ accumulates due to termination. The decrease is much less pronounced for small particles because of a lower extent of termination, and thus the accumulation of T$^\bullet$ with increasing conversion is weaker. As a consequence, N remains almost constant for $d = 20$ nm.

In bulk, more than 15 S units are added in each activation−deactivation cycle when the conversion is less than 1%, i.e. polymer of molecular weight in excess of 1500 is formed in one single activation−deactivation cycle (Figure 10). This may suggest that it is impossible to prepare polymer of low M_n, e.g, 2000, and low M_w/M_n using S/TEMPO at 125 °C in bulk. However, only approximately one-third of the total number of PT will undergo an activation−deactivation cycle in the first 1% conversion (approximately 3 min based on the bulk model and rate parameters employed in the current study, with $[T^\bullet]_0 = 0$), and the majority of chains will thus start growing with less than 15 units added in the first activation−deactivation cycle. Moreover, in practice it is difficult to purify an alkoxyamine from its nitroxide,[47] and thus [T$^\bullet$] is rarely completely zero and N is lower than that predicted based on $[T^\bullet]_0 = 0$.

Comparison with Experiment. TEMPO-mediated radical polymerization of S mainly proceeds in the stationary state (i.e., the time taken to reach the stationary state is very short relative to the polymerization time, unlike in NMP systems with higher K[2]), and as such R_p is independent of the alkoxyamine concentration and equal to the rate of thermal polymerization of S,[2,21] and differences in alkoxyamine concentration is thus not a concern when comparing experiments. In most reported cases, S/TEMPO miniemulsion polymerizations using macroinitiator (PT),[22,23] benzoyl peroxide (BPO)/TEMPO,[25,26] or potassium persulfate (KPS)/TEMPO[25,27−29] result in R_p values very similar to in bulk.[21] However, Pan et al.[24] observed that in TEMPO-mediated S polymerization in miniemulsion at 125 °C relying entirely on thermal initiation (no initiator added), the initial R_p was approximately 50% higher in bulk than in the miniemulsion (no information given on particle size), and they attributed this to geminate termination of thermally generated radicals in miniemulsion. Cunningham et al.[27] speculated that compartmentalization effects may be responsible for higher R_p in S/KPS/TEMPO miniemulsion polymerizations at 135 °C for $d_n = 96$ nm compared to 216 nm at different [KPS] (three times

higher for $d_n = 96$ nm) but the same [KPS]/[TEMPO]. Cunningham and co-workers[48,49] also reported that there was a strong apparent dependence of R_p in S/PT miniemulsion on the amount of the surfactant sodium dodecylbenzenesulfonate (SDBS). Despite the different SDBS concentrations, the particle size distributions were "nearly identical" with a "mean diameter" of 150 nm, and it was speculated that SDBS or SDBS impurities consume nitroxide, thus resulting in an increase in R_p.[48] The latter example illustrates that when comparing R_p in miniemulsion and bulk, it is not possible to ascribe any differences entirely to compartmentalization effects because there are other inherent differences between homogeneous and dispersed systems such as nitroxide partitioning,[11,12] exit/entry of monomeric radicals derived from chain transfer to monomer,[9] the Laplace pressure inside the particles,[50] and also less understood effects of the interface between particle and aqueous phase.[51,52] On the basis of the partitioning coefficient of TEMPO between S and water ($[TEMPO]_S/[TEMPO]_{aq} = 98.8$[45]) and assuming phase transfer equilibrium,[12] TEMPO partitioning should not have a significant effect on R_p.[11] However, Cunningham et al. reported that addition of water to the miniemulsion led to somewhat higher R_p and attributed this to TEMPO partitioning.[28]

The present modeling and simulations indicate that strong effects of compartmentalization in the S/TEMPO system (using "normal" reactant concentrations) only occur for particles with diameters less than approximately 110 nm. The particle size distribution in a miniemulsion is normally relatively broad, and thus even if the number-average particle diameter is equal to say 80 nm, most of the polymer would form in larger particles of the distribution (which constitute a significant mass fraction),[22] and thus compartmentalization effects would not be expected to be important. Within this context, it would be of interest to examine microemulsion NMP ($d \approx 10-30$ nm; there are to date no reports of microemulsion NMP to the best of our knowledge). For such small particles, the present model predicts that the effects of compartmentalization are lower R_p, lower M_w/M_n, and higher degree of livingness than in bulk.

Conclusions

Modeling and simulations of nitroxide-mediated radical polymerization in a dispersed system have been performed for styrene/2,2,6,6-tetramethylpiperidinyl-1-oxy (TEMPO) (for a TEMPO-terminated polystyrene macroinitiatior with $[TEMPO]_0 = 0$) at 125 °C using modified Smith−Ewart equations, whereby compartmentalization of both propagating radicals and nitroxide is accounted for. The effects of thermal initiation were carefully investigated, but phase transfer events were not included in the model.

When the particle diameter (d) is less than approximately 60 nm, a reduction in d leads to lower polymerization rate (R_p), lower polydispersity and higher degree of livingness. This is because of the effect of particle volume on the pseudo-first-order rate coefficient for deactivation (the confined space effect), which increases with decreasing particle size. Consequently the bulk value of the equilibrium constant (for the equilibrium between active and dormant chains) does not apply in a sufficiently compartmentalized system. The effect of compartmentalization on deactivation is stronger than that of segregation of propagating radicals, which in itself leads to less bimolecular termination and higher R_p. The polymerization is unaffected by thermal initiation for $d < 60$ nm because of rapid geminate termination of thermal radicals generated in pairs.

A particle size region exists where R_p at low conversion (< approximately 4%) is higher (by approximately 50% at $d = 70$ nm) than in the corresponding bulk system. In this region, the segregation effect on propagating radicals (leading to a lower rate of bimolecular termination) is stronger than the confined space effect on the deactivation rate (leading to a higher deactivation rate), the net effect being an increase in R_p.

The results illustrate that it is pivotal to consider compartmentalization of both propagating radicals and nitroxide in dispersed polymerization systems. The completely different conclusions previously put forward by Butte et al.[13] and Charleux[34] have their origin in Charleux not including compartmentalization of nitroxide in the model, whereas Butte et al. did. In the styrene/TEMPO system at 125 °C, significant compartmentalization effects occur for particles with diameters less than approximately 110 nm, and the present results thus have implications for emulsion polymerization, miniemulsion polymerization, and obviously microemulsion polymerization processes. Furthermore, preliminary investigations indicate that the effects described are of a general nature and are also operative in atom transfer radical polymerization in dispersed systems. Work is currently underway to investigate other NMP systems, as well as ATRP systems, using the framework developed in the present study.

Acknowledgment. This work was partially supported by the Support Program for Start-ups from Universities (No. 1509) from the Japan Science and Technology Agency (JST), and the Grant-in-Aid for Scientific Research (Grant 17750109) from the Japan Society for the Promotion of Science (JSPS).

References and Notes

(1) Matyjaszewski, K. *Advances in Controlled/Living Radical Polymerization*; American Chemical Society: Washington, DC, 2003.
(2) Goto, A.; Fukuda, T. *Prog. Polym. Sci.* **2004**, *29*, 329−385.
(3) Cunningham, M. F. *Prog. Polym. Sci.* **2002**, *27*, 1039−1067.
(4) Qiu, J.; Charleux, B.; Matyjaszewski, K. *Prog. Polym. Sci.* **2001**, *26*, 2083−2134.
(5) Okubo, M.; Minami, H.; Zhou, J. *Colloid Polym. Sci.* **2004**, *282*, 747−752.
(6) Kagawa, Y.; Minami, H.; Okubo, M.; Zhou, J. *Polymer* **2005**, *46*, 1045−1049.
(7) Zetterlund, P. B.; Alam, Md. N.; Minami, H.; Okubo, M. *Macromol. Rapid Commun.* **2005**, *26*, 955−960.
(8) Alam, Md. N.; Zetterlund, P. B.; Okubo, M. *Macromol. Chem. Phys.*, in press.
(9) Gilbert, R. G. *Emulsion Polymerization: A Mechanistic Approach*; Academic Press: London, 1995.
(10) Qiu, J.; Pintauer, T.; Gaynor, S. G.; Matyjaszewski, K.; Charleux, B.; Vairon, J.-P. *Macromolecules* **2000**, *33*, 7310−7320.
(11) Zetterlund, P. B.; Okubo, M. *Macromol. Theory Simul.* **2005**, *14*, 415−420.
(12) Ma, J. W.; Cunningham, M. F.; McAuley, K. B.; Keoshkerian, B.; Georges, M. K. *Macromol. Theory Simul.* **2002**, *11*, 953−960.
(13) Butte, A.; Storti, G.; Morbidelli, M. *DECHEMA Monogr.* **1998**, *134*, 497−507.
(14) Butte, A.; Storti, G.; Morbidelli, M. *Macromol. Theory Simul.* **2002**, *11*, 37−52.
(15) Prescott, S. W.; Ballard, M. J.; Gilbert, R. G. *J. Polym. Sci.; Part A: Polym. Chem.* **2005**, *43*, 1076−1089.
(16) Luo, Y.; Wang, R.; Yang, L.; Li, B.; Zhu, S. *Macromolecules* **2006**, *39*, 1328−1337.
(17) Georges, M. K.; Veregin, R. P. N.; Kazmaier, P. M.; Hamer, G. K. *Macromolecules* **1993**, *26*, 2987−2988.
(18) Hawker, C. J.; Bosman, A. W.; Harth, E. *Chem. Rev.* **2001**, *101*, 3661−3688.
(19) Matyjaszewski, K.; Xia, J. *Chem. Rev.* **2001**, *101*, 2921−2990.
(20) Moad, G.; Rizzardo, E.; Thang, S. H. *Aust. J. Chem.* **2005**, *58*, 379−410.
(21) Fukuda, T.; Terauchi, T.; Goto, A.; Ohno, K.; Tsujii, Y.; Miyamoto, T.; Kobatake, S.; Yamada, B. *Macromolecules* **1996**, *29*, 6393−6398.
(22) Pan, G.; Sudol, E. D.; Dimonie, V. L.; El-Aasser, M. S. *Macromolecules* **2001**, *34*, 481−488.
(23) Pan, G.; Sudol, E. D.; Dimonie, V. L.; El-Aasser, M. S. *Macromolecules* **2002**, *35*, 6915−6919.

(24) Pan, G.; Sudol, E. D.; Dimonie, V. L.; El-Aasser, M. S. *J. Polym. Sci.; Part A: Polym. Chem.* **2004**, *42*, 4921−4932.
(25) Cunningham, M. F.; Tortosa, K.; Ma, J. W.; McAuley, K. B. *Macromol. Symp.* **2002**, *182*, 273−282.
(26) Prodpran, T.; Dimonie, V. L.; Sudol, E. D.; El-Aasser, M. S. *Macromol. Symp.* **2000**, *155*, 1−14.
(27) Cunningham, M. F.; Xie, M.; McAuley, K. B.; Keoshkerian, B.; Georges, M. K. *Macromolecules* **2002**, *35*, 59−66.
(28) Cunningham, M.; Lin, M.; Buragina, C.; Milton, S.; Ng, D.; Hsu, C. C.; Keoshkerian, B. *Polymer* **2005**, *46*, 1025−1032.
(29) Keoshkerian, B.; MacLeod, P. J.; Georges, M. K. *Macromolecules* **2001**, *34*, 3594−3599.
(30) Butte, A.; Storti, G.; Morbidelli, M. *Macromolecules* **2001**, *34*, 5885−5896.
(31) Smith, W. V.; Ewart, R. H. *J. Chem. Phys.* **1948**, *16*, 592−599.
(32) Yamada, B.; Zetterlund, P. B. In *Handbook of Radical Polymerization*; Matyjaszewski, K., Davis, T. P., Eds.; Wiley-Interscience: New York, 2002.
(33) Luo, Y.; Schork, F. J. *J. Polym. Sci.; Part A: Polym. Chem.* **2002**, *40*, 3200−3211.
(34) Charleux, B. *Macromolecules* **2000**, *33*, 5358−5365.
(35) Russell, G. T. *Aust. J. Chem.* **2002**, *55*, 399−414.
(36) Goto, A.; Terauchi, T.; Fukuda, T.; Miyamoto, T. *Macromol. Rapid Commun.* **1997**, *18*, 673−681.
(37) Buback, M.; Gilbert, R. G.; Hutchinson, R. A.; Klumperman, B.; Kuchta, F. D.; Manders, B. G.; O'Driscoll, K. F.; Russell, G. T.; Schweer, J. *Macromol. Chem. Phys.* **1995**, *196*, 3267−3280.
(38) Buback, M.; Kowollik, C.; Kurz, C.; Wahl, A. *Macromol. Chem. Phys.* **2000**, *201*, 464−469.
(39) Hui, A. W.; Hamielec, A. E. *J. Appl. Polym. Sci.* **1972**, *16*, 749−769.
(40) Zetterlund, P. B.; Yamazoe, H.; Yamada, B.; Hill, D. J. T.; Pomery, P. J. *Macromolecules* **2001**, *34*, 7686−7691.
(41) Zetterlund, P. B.; Yamauchi, S.; Yamada, B. *Macromol. Chem. Phys.* **2004**, *205*, 778−785.
(42) Heath, M. T. *Scientific Computing, An Introductory Survey*; 2nd ed.; McGraw-Hill: New York, 2002.
(43) Ma, J. W.; Cunningham, M. F.; McAuley, K. B.; Keoshkerian, B.; Georges, M. K. *Chem. Eng. Sci.* **2003**, *58*, 1163−1176.
(44) Cunningham, M. F.; Tortosa, K.; Lin, M.; Keoshkerian, B.; Georges, M. K. *J. Polym. Sci., Part A: Polym. Chem* **2002**, *40*, 2828−2841.
(45) Ma, J. W.; Cunningham, M. F.; McAuley, K. B.; Keoshkerian, B.; Georges, M. K. *J. Polym. Sci.; Part A: Polym. Chem.* **2001**, *39*, 1081−1089.
(46) Ballard, M. J.; Napper, D. H.; Gilbert, R. G. *J. Polym. Sci.; Polym. Chem. Ed.* **1984**, *22*, 3225−3253.
(47) Aldabbagh, F.; Dervan, P.; Phelan, M.; Gilligan, K.; Cunningham, D.; McArdle, P.; Zetterlund, P. B.; Yamada, B. *J. Polym. Sci.; Part A: Polym. Chem.* **2003**, *41*, 3892−3900.
(48) Cunningham, M. F.; Lin, M.; Keoshkerian, B. *JCT Res.* **2004**, *1*, 33−39.
(49) Lin, M.; Cunningham, M. F.; Keoshkerian, B. *Macromol. Symp.* **2004**, *206*, 263−274.
(50) Zetterlund, P. B.; Okubo, M. *Macromol. Theory Simul.* **2006**, *15*, 40−45.
(51) Nakamura, T.; Zetterlund, P. B.; Okubo, M. *Macromol. Rapid Commun.* **2006**, *27*, 2014−2018.
(52) Tauer, K.; Oz, N. *Macromolecules* **2004**, *37*, 5880−5888.

MA060841B